JOINT EUROPEAN TORUS JET

JET-P(89)63

J. Blum, B. Keegan, E. Lazzaro, J. O'Rourke
and Y. Stephan

Problems and Methods of Self Consistent Reconstruction of Tokamak Equilibrium Profiles from Magnetic and Polarimetric Measurements

Problems and Methods of Self Consistent Reconstruction of Tokamak Equilibrium Profiles from Magnetic and Polarimetric Measurements

J. Blum[1], B. Keegan, E. Lazzaro, J. O'Rourke
and Y. Stephan[2]

JET Joint Undertaking, Culham Science Centre, OX14 3DB, Abingdon, UK

[1]*Université de Grenoble, B.P. 53X, 38041 Grenoble, Cedex, France*
[2]*CISI, C.E.N., B.P.1, 13108 Saint-Paul-lez-Durance, France*

Preprint of a paper to be submitted for publication in
Nuclear Fusion

Problems and Methods of Self Consistent Reconstruction of Tokamak Equilibrium Profiles from Magnetic and Polarimetric Measurements

J. Blum*, E. Lazzaro, J. O'Rourke, B. Keegan and Y. Stephan**

JET Joint Undertaking, Abingdon, Oxon. OX14 3EA, UK.
*Université de Grenoble, B.P. 53X, 38041 Grenoble, Cedex, France.
**CISI, C.E.N., B.P.1, 13108 Saint-Paul-lez-Durance, France.

ABSTRACT

Recent advances in experimental measurements of magneto-optic properties of tokamak plasmas and progress in formulation of numerical algorithms for the analysis of magnetic data have allowed the self consistent determination of the current density in the JET tokamak, in ohmic and additionally heated discharges. An investigation of the numerical response of a model with finite parametrisation to the uncertainties of the discrete data available, is carried out. The error propagation is analysed for various types of discharges and results on the safety factor profile are presented.

INTRODUCTION

The measurement of the rotation of the polarisation angle of infrared radiation crossing the meridian cross section of a circular plasma along several chords, has been proposed [1] and used to obtain the poloidal field profile through Abel inversion techniques [2-4]. In these cases the procedure is almost exact, because for large aspect ratio machines at moderate values of β_p, the geometry of the magnetic surfaces and the position of the magnetic axis can be assumed to be known [2-4]. However, rarely consistency checks are made between the results of optical methods and global magnetic measurements, with the exception of the total current, generally used to scale the results.

In plasmas of tight aspect ratio and strongly non circular cross section [5-11] Abel inversion techniques are not directly or exactly applicable, and at best iteration

procedures can be devised, based on the previous (magnetic) reconstruction of the flux surface geometry [4,12]. Predictive calculations of the equilibrium may be used, having as input prescribed current and pressure profiles. Due to the arbitrariness of the choices to be made, this procedure has hardly ever been adopted except for sensitivity studies. The formulation of regularised versions of the ill posed inverse equilibrium problem has been developed in recent years [13-17]. These techniques are based on the optimisation of the current distribution which best fit the available external measurements (magnetic, and polarimetric), and are compatible with the force balance condition.

Extensive work on equilibrium identification based only on external magnetic signals has led to the general consensus that only a limited amount of information on the poloidal field (or current, or safety factor) profile can be derived, in the case of significantly elongated plasmas [5-17]. The information retrieved generally consists of up to three numerical parameters related to physical quantities such as β_p, ℓi, q(a), and the geometry of the boundary.

It is arguable whether it is worthwhile to tackle much more complicated 'composite' problems which make use of heterogeneous data, to reduce the uncertainty in the central value of the safety factor or its higher order profile features, from indirect calculations, while some more direct measurements of the field distribution, such as the Stark effect and the polarization spectroscopy of impurity lines [18,19] are becoming technically available.

It is however of considerable interest to attempt to answer the fundamental question of how to formulate in minimal form an inverse problem for the plasma MHD equilibrium, which possesses a stable unique solution, for given data. Recent results of numerical reconstruction of equilibrium pressure and current profiles using exact data from other numerical simulations [16] have been published. However the results offered in these works are not fully conclusive for the analysis of experimental data.

Given the variety of experimental observations with which the solution of the problem must be compatible and consistent, the first task is to define unequivocally the equilibrium model and to isolate the information *a priori* necessary to identify it. The second question is the definition of selection criteria, or constraints to which the approximate solution of the problem must be subject, to approach as close as possible the characteristics of the true solution. The choice of constraints should naturally follow from clear physical and mathematical requirements, rather than from empirical approaches.

In the following we present the discussion and the results of numerical algorithms developed [13-15] for JET to solve the axisymmetric isotropic Grad-Shafranov equation without flow, within a 'nested' set of inverse problems involving an increasing number of experimental data.

The response of the algorithm to the uncertainties of the data and to the 'slackness' or 'degrees of freedom' of the model is studied for typical discharges in order to evaluate the technical error bars expected from the procedure.

In particular the question of the optimal smoothness (or number of free parameters) in the models of average current and pressure profiles is addressed, keeping in mind that a well posed (stable) pseudo-inverse problem should be suitably overdetermined.

An excessive flexibility of the 'model' may lead to underdetermination with consequent unphysical response to the data. In Section I a succinct formulation is presented of the general aspects of the problem. Section II specialises to the case for which the algorithm in use at JET was developed. Section III presents the sensitivity and response curves appropriate for two typical classes of discharges (ohmic, and H-modes) leading to the estimate of error bars on several physical parameters.

I. GENERAL STRUCTURE OF MHD EQUILIBRIUM RECONSTRUCTION PROBLEM WITH DISCRETE DATA

The simplest equilibrium model for a tokamak is described by the Grad-Shafranov equation for the magnetic stream function ψ:

$$R^2 \underline{\nabla} \bullet \left[R^{-2} \underline{\nabla} \psi\right] = -\mu_o R J_\phi(R, \psi) \tag{1}$$

in which the source term (current density) is specified in terms of the pressure gradient function p', the paramagnetic flux function F and the radial coordinate R, as:

$$J_\phi(R, \psi) = R \frac{dp}{d\psi} + \left(\frac{1}{\mu_o R}\right) F \frac{dF}{d\psi}. \tag{2}$$

For any choice of p and F and certain boundary conditions for ψ a 'direct' problem is constructed, which establishes a mapping between the current profile J_ϕ, and a set of calculated results, f_k, (k = 1, ... N), i.e. numbers $f_k(J_\phi)$, which are functionals of J_ϕ which can be compared with the measurements vector $\{g_k\}$. In the present case, for instance a set of functionals is

$$f_i = \left(\frac{1}{R} \frac{\partial \psi}{\partial \upsilon}\right)_i i - 1,...18 \ \ and \ \ \alpha_i = \int_{L_i} \frac{n(\psi)}{R} \frac{\partial \psi}{\partial R} dz, \quad j = 1,...6.$$

where $(\frac{\partial \psi}{\partial \nu})_i$ are the values of the normal derivative of ψ on the vacuum vessel and N = 24.

In these terms the problem of 'plasma equilibrium identification' is an inverse problem for Eq. (1), which aims at recognising the mapping relating the set (discrete and finite) of experimental measurements g_k expressible as functionals of $J_\phi(R,\psi)$, to the field function ψ and finally to a set of characteristic physical parameters of the current profile. The problem has similarities with that of reconstructing a distribution from a set of moments. A complete set for a free boundary problem however does not exist [8].

Ignoring the errors in the data, the basic form of a (linearised) inverse problem in the normalised variable $\overline{\psi}$, ($0 < \overline{\psi} < 1$) could be posed in the form: **"given a class of functions X (generally spanning a Hilbert space L_{01}^2 on the interval $0 < \overline{\psi} < 1$), and given a set f_n of continuous linear functionals defined on X, and a set of values g_n (data vector) of these functionals, find in X a function J_ϕ such that:**

$$f_n\left(J_\phi\left(R,\overline{\psi}\right)\right) = g_n \qquad \textbf{(3)"}$$

On the basis of the Riesz representation theorem it can be proved [20-22] that, if the N f_n are linearly (functionally) independent, there always exists a unique solution J* of minimal norm in X (normal solution) to the problem.

The solution is orthogonal to the subspace of the functions which annihilate the f_n. This means that a finite data vector allows only the determination of the projection J* of the unknown object J_ϕ on a subspace X_N and that the component of J_ϕ orthogonal to X_N is 'invisible'. For finite N the formal computation of J* is a well posed problem [20], but for large N it may lack numerical stability because it is the projection on a finite dimensional space of an **ill posed** problem which lacks continuous dependence on the data. By adding more and more experimental data g_n, as a consequence of the errors in the measurements, or by the very definitions of the functionals, not all the functionals are effectively independent and no more independent information about J_ϕ is provided [20].

The presence of noise limits the effectively independent functionals to a number M << N and therefore the optimum number of degrees of freedom of the problem must not exceed M [16,20]. M depends both on the noise and on the structure of functionals and of the space X.

In the interval $0 < \overline{\psi} < 1$ the choice of the functions X could be restricted by *a priori* knowledge of some properties of p' and FF', (i.e. symmetries and support and continuity properties). On the basis of Weierstraβ approximation theorem it is in general appropriate to use elements of a complete set of polynomials, which obey the boundary conditions in $\overline{\psi}$, thereby reducing the problem to the evaluation of

their coefficients [20,21]. A purely numerical reconstruction of local values of the current density can remove the bias of an analytical choice.

The full problem to be solved is actually nonlinear. For these reasons it is convenient to cast the identification problem in the form of a constrained least squares fit of the data which aims at minimising the quantity:

$$\Phi = \sum_{k=1}^{N} w_k |f_k - g_k|^2 + \mu\Omega(J_\phi) \tag{4}$$

under the constraint of fulfilling Eq. (1) with appropriate boundary conditions for a free contour configuration [15] and a parameterised model with a number of free parameters M < N [13-15].

Each term k of the sum from 1 to N represents the discrepancy between the calculated and measured values of experimental data, with weight w_k, and $\Omega(J)$ is a regularisation functional of the Tikhonov type [20], with parameter μ, which restricts the class of solutions to those with a chosen, physically meaningful, degree of smoothness.

It can be proved [20] that for a suitable value of μ, the generalised solution of the constrained least square problem converges, for vanishing errors in the data, to noise free normal solution which is an M dimensional image of the true solution.

The constrained minimum problem (4) can be tackled with techniques using generalised Lagrange multipliers, as described in Ref. [15]. It should be noted that the success of the procedure depends on the convexity of the functional Φ with respect to the control variables: adding terms which are not clearly related to the equilibrium problem may destroy the required properties. In the references quoted in this paragraph, one can find the formal proof of the statements on which the reconstruction methods are founded.

In the following section, results are presented of the concrete application in the case of magnetic, polarimetric (Faraday rotation), and pressure measurements in JET, to obtain estimates of the resolution limit and of the error propagation of this procedure in real situations.

II. OPTIMISATION OF CURRENT DENSITY PROFILE

The specific numerical techniques used at JET for the inverse equilibrium problem are described elsewhere [15]. Here it is only necessary to specify the finite parametrisation model of the toroidal current distribution J_ϕ, and the form of the objective function Φ.

The current density has the general structure

$$J_\phi = \lambda\left\{R\beta A[a_1, a_2 \cdots a_m] + (1-\beta)B[b_1, b_2 \cdots b_m]/R\right\} \tag{5}$$

with 2m + 1 free parameters a_k, b_k, β. The scalars a_k and b_k represent the values of the functions A and B at m grid points of the normalised magnetic flux function $\overline{\psi}$ = $(\psi_{axis} - \psi)/(\psi_{axis} - \psi_{bound})$, with ψ_{axis} and ψ_{bound} the values of ψ on axis and at the plasma boundary, and $0 < \overline{\psi} < 1$. The functions A and B are not specified analytically in any way, but are determined in a pure numerical way under suitable numerical constraints of regularity, discussed in what follows, and typical of function approximation theory. In the applications presented here m = 10 and A = B and therefore only the current $\langle J_\phi \rangle$ averaged over a magnetic surface can be identified. These control parameters are determined by a numerical technique, first reported in Ref. [14], from the minimisation of Φ; λ is a state variable related to the normalisation of J_ϕ to the total current I_p; J_ϕ is here assumed, as customary, to vanish at the free plasma boundary, where plasma-vacuum interface conditions are imposed as continuity of magnetic flux and tangential field. The measurements available at JET are 14 values of the magnetic flux ψ on the vessel contour, providing a Dirichlet boundary condition for Eq. (1) , 18 values of the tangential field $B_\tau = \frac{1}{R}\frac{\partial \psi}{\partial v}$ around the vessel cross section, 6 channels of interferometric and polarimetric measurements, one diamagnetic flux measurement and a 45 point electron pressure profile measurement [13,23].

On the basis of these measurements the following objective functional has been used,. for a self consistent determination of the equilibrium:

$$\Phi(\psi,\lambda,a_i,c_i,\beta)=\frac{1}{2}\sum_{k=1}^{18}\left|(1/R)\left(\frac{\partial\psi}{\partial\upsilon}\right)_k-f_k\right|^2+\frac{1}{2}\sum_{k=1}^{6}W_F\left[c\int_{L_k}\left(\frac{n\partial\psi}{R\partial R}\right)d\ell-\alpha_{F_k}\right]^2$$

$$+\frac{1}{2}\sum_{k=1}^{6}W_n\left[\int_{L_k}n_C d\ell-N_k\right]^2+\frac{1}{2}w_p\left[\int_0^1 p_C ds-\int_0^1 p_m ds\right]^2+\frac{1}{2}w_{Rn}\int\left[\frac{\partial^2 n}{\partial\psi^2}\right]^2+\frac{1}{2}w_{Rj}\int\left[\frac{\partial^2 A}{\partial\psi^2}\right]^2 \quad (6)$$

The first term of (6) describes the fitting of the external tangential field measurements $\frac{1}{R}\frac{\partial\psi}{\partial\nu}$ where $\frac{\partial\psi}{\partial\nu}$ indicates the derivative of ψ normal to the boundary. The second term represents the discrepancy between the calculated Faraday rotation angle $\alpha = C\int_{L_k}\frac{n}{R}\frac{\partial\psi}{\partial R}d\ell$ with $C = 2.62\times10^{-17}\lambda^2[cm^2]$ and the measured value α. It should be noted that in the present application to JET the evolution of the wave polarisation is adequately described by α, neglecting the Cotton-Mouton variation of the ellipticity of the polarisation since even in the presence of considerable birefringence the relation $\alpha \sim \int n\, B d\ell$ is fulfilled [4]. The third term represents the discrepancy of the density line integral measurements N_k, and the fourth the pressure profile measurements (in the latter two terms subscripts c, m, stand for calculated and measured values). The last two terms describe regularisation terms Ω for the average current density and the particle density, which is assumed to be a flux function. The density profile is also determined self consistently through its local values c_i, in the same way as the current. In total in the present application there are 10 free local values of the surface averaged current profile and 10 free local values of the density profile. An extension of Φ has also been provided, but not tested, in which the location of the q = 1 rational surface is enforced, as determined from the soft X-ray inversion radius.

The weight of each term of the objective function Φ is related to the inverse of the square of the variance of the measurements. Indicative values of the accuracy δ of measurements in JET are shown in Table I. Therefore in a sound application of the algorithm, there is no arbitrary choice on variation of the weights.

However, a preliminary study is necessary to validate the procedure, and to gain insight into the response of the algorithm to the information provided by possibly heterogeneous data.

Accordingly, and only for the purpose of testing the algorithm, we must check, by varying W_F and W_N, the effect of enforcing into the equilibrium reconstruction the fitting of the polarimetric and interferometric data, and their consistency with the magnetic data.

Let C, and M indicate generically the calculated and measured quantities, then each term of the objective function ϕ can be related to a root mean square relative error (r.m.s.) defined here as

$$\varepsilon = \sqrt{\sum_k \frac{(C_k - M_k)^2}{\sum M_k^2}}$$

or to a standard definition of the statistic

$$\chi_n^2 = \sum_k \frac{(C_k - M_k)^2}{n\sigma^2}$$

with n degrees of freedom. It is expected that, for instance the plots versus W_F of the magnetic, interferometric and polarimetric ε, should indicate a compatibility range of the algorithm, in which the data of the various diagnostics are fitted within their error bars.

Naturally the performance of the algorithm is acceptable only if the range of compatibility contains the value of W_F corresponding to the experimental estimate of the standard deviation of the Faraday rotation data.

The numerical determination of J_ϕ as defined in Eq. (5), and of the particle density profile $n(\overline{\psi})$ appearing in expression (6), are, ideally, free from biased choices of functional dependence on $\overline{\psi}$. However, the task of determining the appropriate degree of smoothness of thes profiles requires extensive numerical tests. To this end it is necessary to consider the behaviour of ε for the magnetic, interferometric and Faraday rotation data fit, as function of the weights W_{RJ} and W_{Rn}, which control

the smoothness of the profiles, using fixed values of W_F and W_N derived from the experimental standard deviation.

It should be carefully noted that large values ($\rightarrow\infty$) of the regularisation parameters W_{RJ}, for instance, correspond to a restriction of $<J_\phi>$ to a linear function of $\overline{\psi}$, which generally does not allow all the data to be fitted within their error bars.

On the contrary, vanishing values of this parameter correspond to physically unacceptable profiles with oscillations, having a scale length comparable with the spacing of the polarimeter lines of sight, which are therefore impossible to resolve.

Therefore controlling the weight of the regularising term of the various experimental profiles to be fitted, is equivalent to finding the 'optimal' number of degrees of freedom of the model. The appropriate estimate of whether the number M of free parameters of the model, applied to N data defines a suitably over-determined problem, is the reduced χ^2_{N-M} value [24]. If this statistic is much smaller than one, the number M of degrees of freedom is too large, and therefore it leads to numerical artifacts, and if χ^2_{N-M} is larger than one, then M is too low and the model is too rigid to fit all the data.

The relation between the weight of the regularising term and the number of degrees of freedom can only be determined a posteriori. In the following section we do not use the reduced χ^2_{N-M} value, but rather the related r.m.s. error, ε, compared directly with the error bars, since a proper statistical χ^2_{N-M} test cannot be strictly applied as many sources of experimental errors in this problem are systematic.

III. RESULTS OF NUMERICAL IDENTIFICATION OF AN OHMIC DISCHARGE

As a reference case we consider the reconstruction provided by the magnetic data (flux loop and pick-up coils signals [17,23]), by keeping only the first and the last term in expression (6).

Fig. 1a shows the flux surface reconstruction with the outline of the JET vessel and the internal structures, including the positions of the measuring pick up

coils and flux loops. The upper insert of Fig. 1a shows the fitting of the calculated tangential field values at the position of the 18 pick up coils. The lower insert shows the comparison between the values of the Faraday rotation angle α calculated from the magnetic reconstruction, and the measured values α_F. It is clear that although the magnetic reconstruction predicts values of α very close to the true ones α_F, the mismatch on the central channels shows a relative insensitivity of the magnetic signals to fine internal details of the current. A consequence of this is however a robust reconstruction which matches within 1% the integral equilibrium relations of Shafranov and Zakharov [25,26] especially if the diamagnetic flux measurement is enforced [17].

Fig. 1b shows the effect of enforcing a self consistent fit of the polarimetric measurements, obtained by giving W_F, W_N and W_{Rn}, in expression (6), non-vanishing values. (Neglecting to enforce the matching of the line integrals of the density to the measurements leads to numerical instability). The inserts of Fig. 1b show that while the fitting of the magnetic signals remains unaltered the fitting of the Faraday rotation angle leads to about 1% change in the geometry and up to 21% in the value of q(0). The accuracy of the polarimetric measurements are therefore crucial for the determination of some details of the current distribution. Fig. 2a shows the surface averaged distribution $<J_\phi>$ plotted vs $\overline{\psi}$ calculated from magnetic data alone and from self consistent magnetic and Faraday data. In Figs. 2b and 2c the same comparison is made for the profiles of $J_\phi(R,Z = 0)$ and q(R) in the equatorial plane. These results are obtained with the weight of the smoothing term, $W_{RJ} = 10^{-5}$. For the typical low β ohmic discharge considered here, the variation of β_p and ℓ_i when the Faraday data are enforced is within the error bars of the data, since the magnetic data are already adequate for these deductions.

The response of the solution to the polarimetric information is illustrated by the scan in W_F presented in Fig. 3a. Here the values of ε for the magnetic, interferometric and polarimetric data are plotted vs $W_F \propto \frac{17\sigma_M^2}{5\sigma_F^2}$, (where σ_M and σ_F

are the standard deviations of the 18 magnetic and 6 Faraday measurements). All the data can be fitted by this algorithm within their error bars, if, $3 < W_F < 30$. The credited experimental estimate for JET is $\sigma_F = \delta \overline{|\alpha_F|} \sim$, where $\overline{|\alpha_F|}$ is the average value of the measurement and δ is the accuracy (see Table I). In this example $\overline{|\alpha_F|} =$ 0.14 [rad], $\sigma_F = 7.10^{-3}$ corresponding to $W_F \approx 10$ which is within the compatibility range.

As a consequence of the new information provided by the polarimetry, the value of q(0) is lowered by up to 21% from its purely magnetic estimate, and it is significantly below one (in this case) However, it is necessary to study the sensitivity of these results, obtained with experimental value of $W_F = 10$, to the smoothing weights W_{RJ} and W_{Rn}, (since the definition of the Faraday functional $\alpha = 2.62 \times 10^{-17}\lambda^2 \int n B_z dZ$ depends on the density profile) in order to assess the bias of the model.

Figs. 4a,b show the behaviour of the r.m.s. ε for the three diagnostics versus W_{RJ} and W_{Rn}, with the other weights fixed to their experimental estimate ($W_F = 10$, $W_N = 10$).

Within the ranges $10^{-6} < W_{Rj} < 10^{-3}$ (Fig. 4a) and $10^{-5} < W_{RN} < 10^{-2}$ (Fig. 4b), the data are fitted within their error bars, and therefore the model does not bias substantially the results.

If a reduced χ^2_{N-M} test could be applied, the number of degrees of freedom M for the current distribution would be 3 or 4 in this range of W_{Rj}.

The relative fitting error at each individual channel of the polarimeter is shown in Fig. 4c for the case with magnetic data above and for the case with $W_F = 10$ (and $W_{RJ} = 10^{-5}$, $W_{Rn} = 10^{-4}$), corresponding to the estimated experimental standard deviation for Faraday data $\sigma_F = 7 \times 10^{-3}$.

The sensitivity of the value of q(0) to the choice of the smoothing parameter W_{Rj} of the current profile, is illustrated in Fig. 4d. Over the operative range $10^{-6} < W_{Rj} < 10^{-3}$ where all the data are fitted, q(0) has a maximum variation of 4.5%. Fig.

4e shows the sensitivity of q(0) to the particle density profile smoothing parameter W_{Rn}. The uncertainty on q(0) associated to the possible choices of W_{Rn} can reach 8.8%. This confirms the fact that with use of polarimetric data, the determination of q(0) may depend crucially on the density profile.

The following figures illustrate the dependence of other global equilibrium parameters on the selection of values of W_{Rj} and W_{Rn} within the range established by minimising the data fitting errors.

The variation with W_{Rj} of the internal inductance ℓ_i and of the Shafranov current profile moments Y_2 and Y_3 [25] is shown in Fig. 4f. The internal inductance and Y_2 vary by about 0.7% while Y_3 seems more sensitive (17%) to the current profile variations in this range. The variations of β_p (Fig. 4g) and ℓ_i appear to be within the error bar of the data, as expected, thoughout the range of W_{Rj}.

The same is true for the dependence of β_p, ℓ_i, Y_2, Y_3 on W_{Rn}, shown in Fig. 4h, 4i

A visual understanding of the effect of selecting a value for W_{Rj} is given by Fig. 5a and 5b. The first shows $<J_\phi>$ vs. $\overline{\psi}$ obtained with the excessively large value $W_{Rj} = 1$. The second shows the same average current obtained with the extremely low value $W_{Rj} = 10^{-7}$. We remark that both these values are outside the "operative range" defined from Fig. 3.

The rest of the analysis of this particular discharge comprises the time evolution of q(0) shown in Fig. 6, obtained both with the measured data and with a 5% systematic perturbation of the Faraday data

Fig. 7a, b show the time evolution of the global parameters β_p, ℓ_i in the same conditions. A systematic error in the polarimetric data produces apparently a constant shift of the value of q(0) which has therefore a range of uncertainty of some 9%. The other parameters are affected similarly.

Having established the width of the response range of the interpretation code to the uncertainties it is possible to estimate the propagation of errors of a quantity

'Y', close to the value obtained with 'experimentally correct' weights W_F, W_N, using the expression

$$\Delta Y = \frac{\partial Y}{\partial W_{Rj}} \Delta W_{Rj} + \frac{\partial Y}{\partial W_{Rn}} \Delta W_{Rn} + \frac{\partial Y}{\partial \alpha_F} \Delta \alpha_F + \frac{\partial Y}{\partial B_\tau} \Delta B_\tau$$

where the last two terms relate to the uncertainty of the experimental measurements of α_F and B_τ. The total error in q(0) due to errors in the data and variations in the smoothing parameters is approximately ± 13%. In Fig. 7c the position and the width of the q = 1 surface is shown for exact and perturbed data, in comparison with the sawteeth inversion radius deduced from soft X-ray emission. The value of q(0) goes below 1 as the sawteeth start. The position of the q = 1 radius and the inversion radius are within the error bar produced by 5% systematic error in α_F. The estimate obtained with the Faraday rotation is consistently somewhat lower than that obtained from magnetics alone. The procedure described can be extended to include a measurement of the pressure profile, obtained from the LIDAR electron pressure profile suitably normalised to the measured diamagnetic β_p. Setting the fourth term of (6) to a non-vanishing value requires knowledge of the variance of pressure data. Results will be presented in a subsequent work. It might be noticed that the value of q(0) obtained from this self consistent procedure embodying the polarimetric measurement, reaches values around 0.7 which are in fair agreement with recent experimental measurements on TEXTOR [3] and TEXT [27] and with analytical estimates [28], and experimental measurements [29] of the critical value of q(0) separating pinch-like relaxed profiles from tokamak-like profiles, (q monotonically increasing). This is in apparent disagreement with other "direct" measurements performed on circular plasmas based on polarisation spectroscopy of heavy impurity emission lines [19].

IV. H-MODE DISCHARGES

For low β_p plasmas (ohmic cases with limiter) the results obtained adding the polarimetric and kinetic information are in good agreement, indicating the basic

compatibility of different 'operative' definitions of the (average) current profile, and a surprisingly good performance of the magnetic reconstruction alone as has been pointed out in [30]. For special types of discharges bounded by a magnetic separatrix, and with finite β_p (H-modes) the algorithm may find difficulties in converging. The results of the magnetic analysis are correct only for the identification of the global quantities and the plasma boundary. The reconstruction of the q profile is strongly influenced by the introduction of the Faraday rotation information. Fig. 8a shows a single X-point JET H-mode equilibrium reconstructed from magnetic data and from data of 4 polarimetric channels with weights $W_{RJ} = 10^{-5}$, $W_{Rn} = 10^{-4}$, $W_F = 10$. Two channels are excluded because the signal was lost due to refraction by the steep density gradients which appear near the plasma boundary during H-modes. Figs. 8b and 8c show the resulting q(R) and J_ϕ profiles, which have clearly non monotonic features. Fig. 8d shows the particle density profile ploted against $\overline{\psi}$, obtained simultaneously with J_ϕ. The non monotonic (hollow) profile is in agreement with independent observations from LIDAR [32]. Figs. 9a and 9b show the sensitivity of response of the algorithm to variations of W_{RJ} and W_{Rn}, as described previously. In this case the value of q(0) is in the range $0.83 < q(0) < 1.13$.

CONCLUSIONS

A very flexible numerical technique has been tested to reconstruct tokamak equilibria from experimental data. The code developed can produce a full equilibrium reconstruction in 25 sec on a Cray computer. The numerical procedure adopted in this work does not rely on any special functional dependence of the current profile with respect to ψ. The error propagation of the method has been reported. The main result is that accurate consistent reconstruction requires high precision data, and that the most reliable results are obtained by suitably restricting the freedom of the model by appropriate regularization. The value of additional information, relevant to the problem, is to resolve ambiguous cases, such as higher β_p equilibria, and to sharpen the estimate of some equilibrium parameter. In

particular, examples of ohmic and H-mode JET discharges have been discussed. It is shown that the use of Faraday rotation in addition to magnetic measurements, produces a reliable self-consistent determination of the q-profile with finite error-bars.

TABLE I

Accuracy δ of the data for JET discharges

Magnetic signals (18 + 14)	: $\delta = \pm 3\%$
Diamagnetic signal	: $\delta = \pm 10\%$
Faraday rotation (≤ 6)	: $\delta = \pm 5\%$
Interferometric density profile (~ 50)	: $\delta = \pm 1\%$
LIDAR electron pressure profile (45)	: $\delta = \pm 20\%$

Acknowledgements

Thanks are due to R. Gill for the inversion radius data and to T. Stringer and the referees for their helpful comments.

References

[1] DE MARCO, F., SEGRE, S.E., Plasma Phys. 14, 245 (1972).

[2] SOLTWISCH, H., in Contr. Fus. and Plasma Phys. Proceed. 111 EPS Conf. Aachen, 1983, paper 7D-1, 123 (1983).

[3] SOLTWISCH, H., Rev. Sci. Instrum. 57, 1939 (1987).

[4] O'ROURKE, J., ET AL., XV EPS Conference, Dubrovnik, Vol. I, 155 (1988); O'ROURKE, J., Plasma Phys. Contr. Fus. 16, 1140, 1139.

[5] LUXON, J.L., BROWN, B.B., Nucl. Fus. 22, 813 (1982).

[6] LAO, L.L., ST.JOHN, H., STAMBAUGH, R.D., ET AL., Nucl. Fus. 25, 1421 (1985).

[7] LAO, L.L., ST.JOHN, H. STAMBAUGH, R.D., ET AL., Nucl. Fus. 25, 1611 (1985).

[8] BRAAMS, B.J., Numerieke Studies van Tokamak Evenwicht en Transport, Ph.D. Thesis, University of Utrecht, 1986.

[9] SWAIN, D.W., NEILSON, G.H., Nucl. Fus. 22, 1015 (1982).

[10] ALLADIO, F., CRISANTI, F., Nucl. Fus. 26, 1164 (1986).

[11] SOLTWISCH, H. AND EQUIPE, T.F.R., Infrared Physics 21, (1981) 287.

[12] ALLADIO, F., CRISANTI, F., JET-TN(87)05.

[13] BLUM, J., GILBERT, J.C., THOORIS, B., Parametric Identification of the Plasma Current Profile from the Magnetic Measurements and Pressure Profile, JET Contract JT3/90008 (1985).

[14] BLUM, J., GILBERT, J.C., LE FOLL, J., THOORIS, B., in Proc. 8th Eur. Conf. on Comput. Phys., Eibsee, Vol.10D, 49 (1986); and J. Blum, Y. Stephan, Rapport EUR-CEA-FC1377 (1989).

[15] BLUM, J., Numerical Simulation and Optimal Control in Plasma Physics, Wiley/Gauthier Villars, Paris 1989.

[16] HOFMANN, F., TONETTI, G., Nucl. Fus. 28 (10), 1871 (1988).

[17] LAZZARO, E., MANTICA, P., Plasma Phys. Contr. Fus. 30 (12), 1735 (1988).

[18] BOILEAU, A., VON HELLERMAN, M., ET AL., JET-P(89)04 submitted to J. Phys. (B).

[19] WROBLEWSKI, D., HUANG, L.K., MOOS, H.W., Phys. Rev. Lett. 15, 1724 (1988).

[20] BERTERO, M., DE MOL, C., PIKE, E.R., Inverse Problems 1, 301 (1985); and 4, 573 (1988).

[21] KOLMOGOROV, A.N., FOMIN, S.V., Elementy teorii funktsii i funktional'nogo analiza, Nauka, Moscow 1980, Chpts. III and VII.

[22] AMERIO, L., Analisi Matematica, Vol. I and Vol. III, UTET Turin, 1982.

[23] TONETTI, G., CHRISTIANSEN, J.P., DE KOCK, L., Rev. Sci. Instrum. 57, 2087 (1987).

[24] BEVINGTON, M., "Data Reduction and Error Analysis for the Physical Sciences", McGraw-Hill, 1969.

[25] ZAKHAROV, L.E., SHAFRANOV, V.D., Sov. Phys. Tech. Phys. 18, 151 (1973).

[26] LAZZARO, E., MANTICA, P., Nucl. Fus. 28, 5913 (1988).

[27] WEST, W.P., THOMAS, D.M., ET AL., Phys. Rev. Lett. 58, 491 (1987).

[28] HASTIE, R.J., Nucl. Fus. 29 (1), 96 (1989).

[29] OSBORNE, T.H., DEXTER, R.N., PRAGER, S.C., Phys. Rev. Lett. 49 (10), 734 (1982).

[30] VABISCHEVICH, P.N., ZOTOV, I.V., Sov. J. Plasma Phys. 14 (11), 759 (1988).

[31] GOWERS, C., BARTLETT, D., BOILEAU, A., ET AL., Proc. 15th EPS Conf. on Contr. Fus. and Plasma Heating, Dubrovnik, Vol. 12B, Part I, 239 (1988).

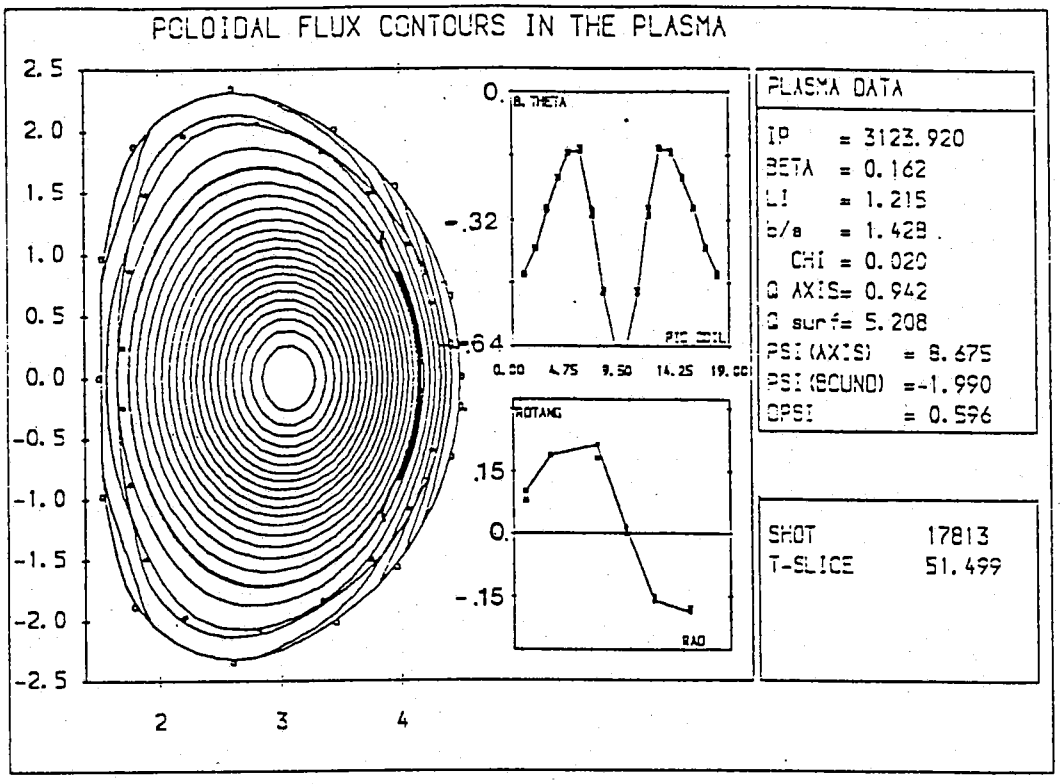

Fig. 1(a) Reconstructed flux surfaces configuration for JET ohmic shot 17813 at $t = 51.5$ from magnetic signals only. The table shows the main plasma parameters: plasma current I_p(kA), β_p, ℓ_i elongation b/a; central and boundary values of q, (q axis and q surf) percentage fit of tangential field, central and edge values of ψ. The inserts show: a) the fitting of the magnetic field coils measured at the 18 pick up coils, and b) the *comparison* of Faraday rotation measurements and calculation along 6 vertical chords.

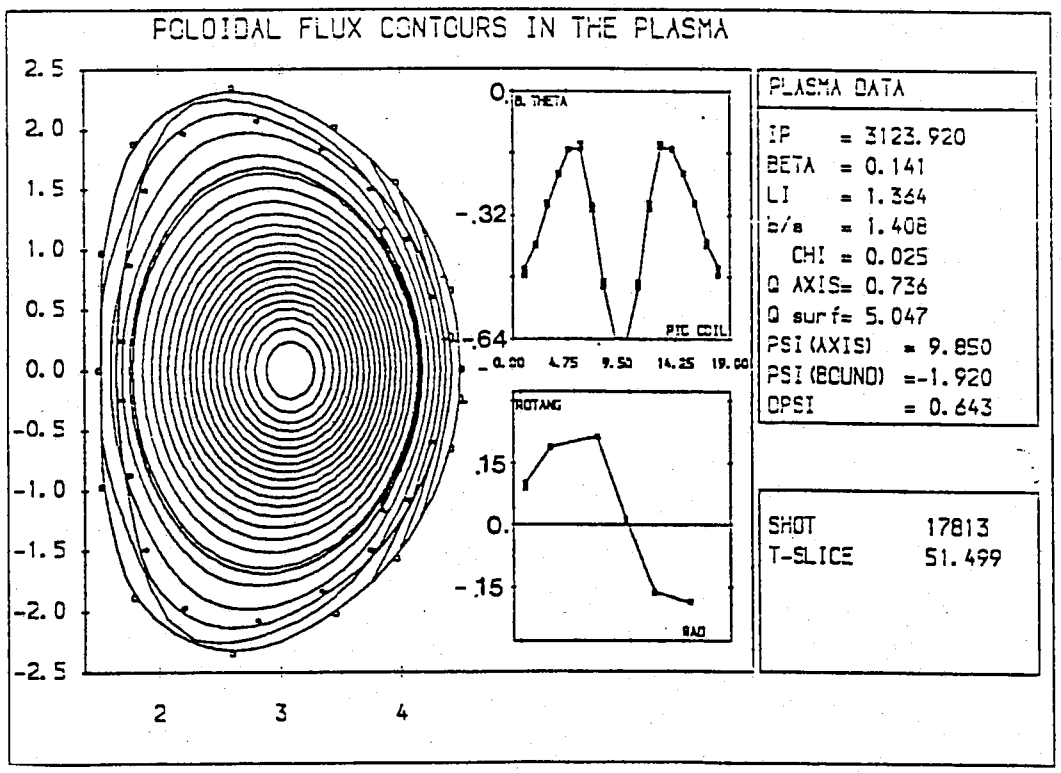

Fig. 1(b) Same as Fig. 1(a) from self consistent use of Faraday data. Insert b) shows the *fitting* of the Faraday rotation measurements.

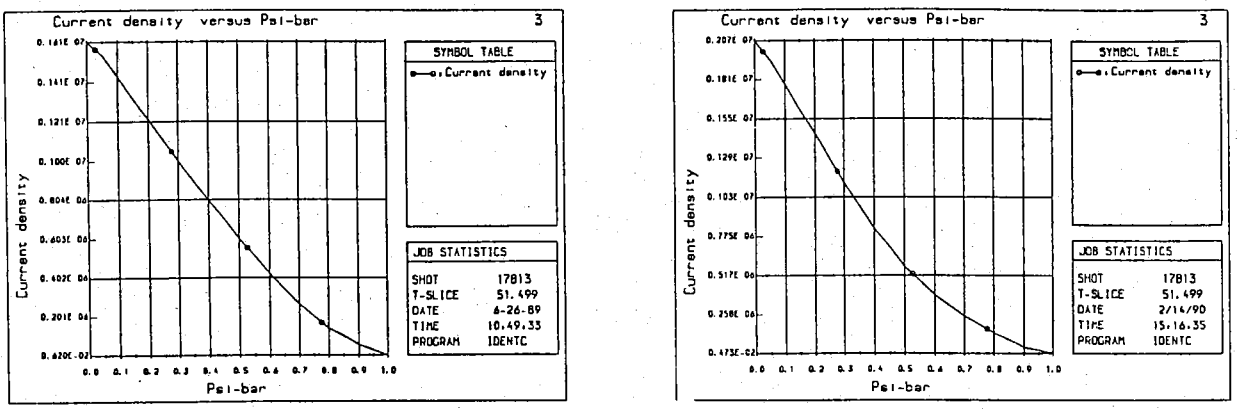

Fig. 2(a) Surface averaged toroidal current $<J_\phi>$ vs $\bar{\Psi}$ obtained from magnetic data only (left) and with Faraday data, with $W_{RJ}=10^{-5}$, $W_F=10$ (right).

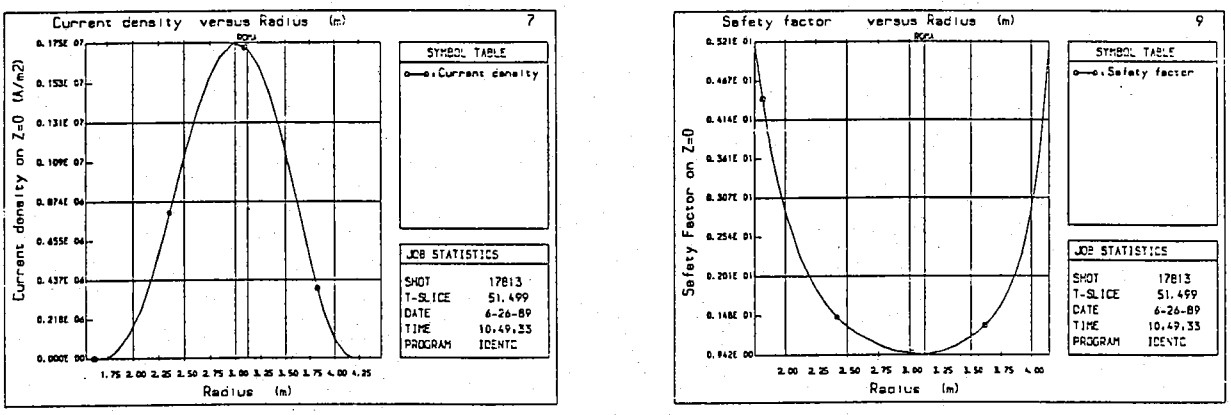

Fig. 2(b) $J_\phi(R,Z=0)$ vs R (left) and $q(R)$ (right) from magnetics alone.

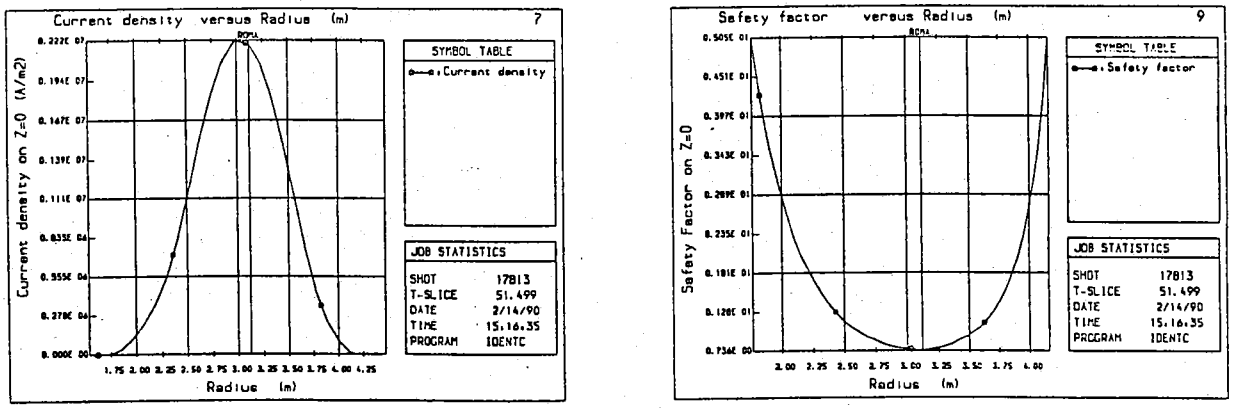

Fig. 2(c) Same as Fig. 2(b) but with magnetics and Faraday rotation.

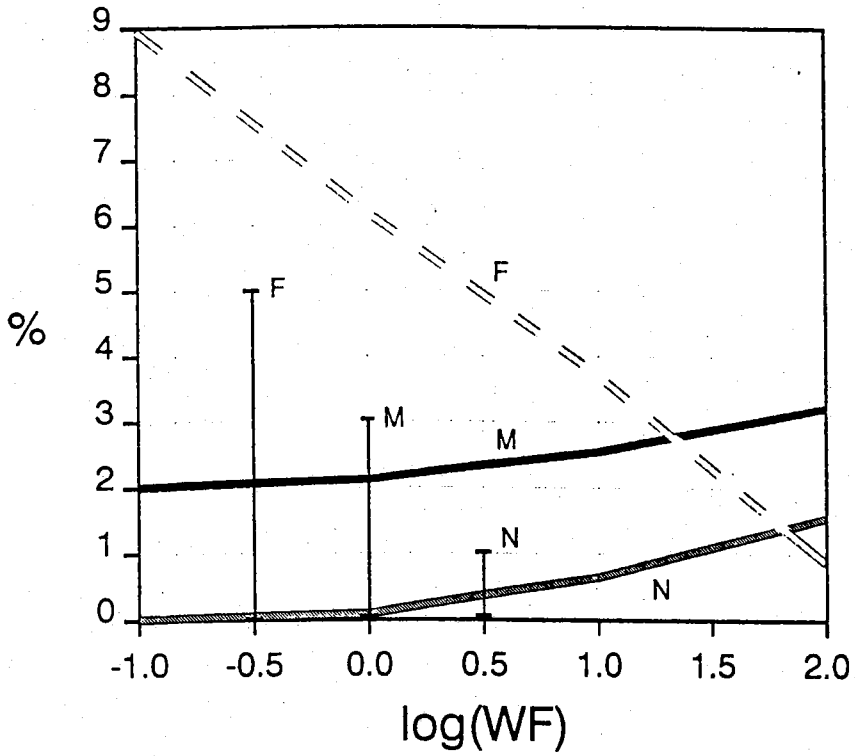

Fig. 3(a) Response to the weight W_F of polarimetric data of the r.m.s. fitting errors ϵ for the Faraday rotation (dashed line), magnetic data (full line), interferometric data (grey line). This plot shows that all the data can be fitted within their error bars (as shown), if the standard deviation of the Faraday measurements corresponds to $3 \leq W_F \leq 30$. The experimentally credited value is $\sigma_F = 7 \times 10^{-3}$ corresponding to $W_F \sim 10$.

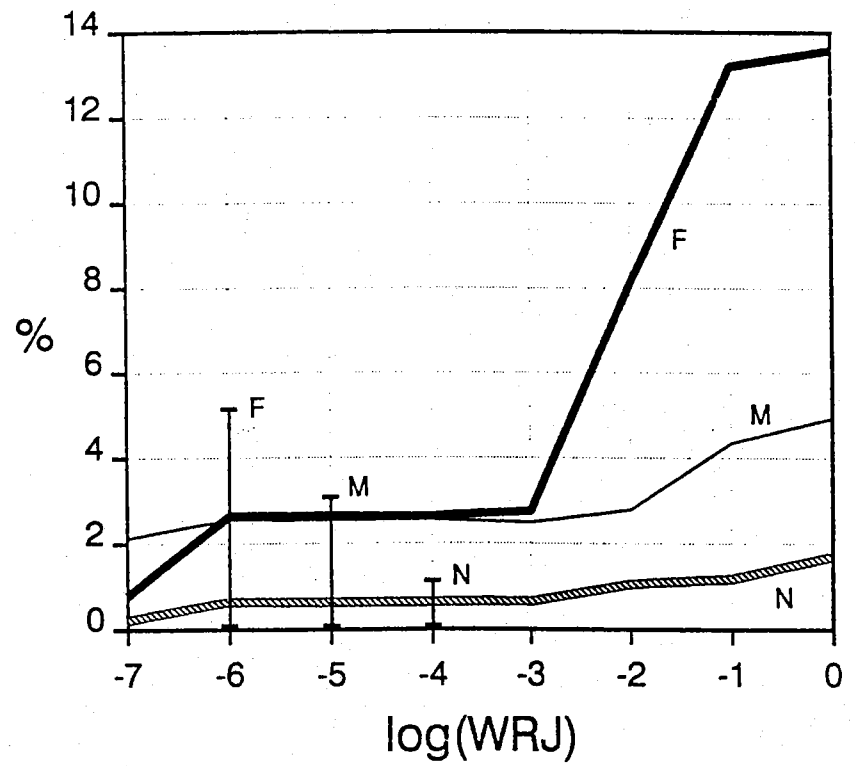

Fig. 4(a) Response of the r.m.s. fitting errors ϵ to the smoothness parameter W_{RJ} of the current, while $W_F = 10$, $W_N = 10$. The full line is the polarimetric (F) fitting error ϵ; experimental error bar 5%. The thin line is for the magnetic (M); experimental error bar 3%. The grey line is for the interferometer (N); experimental error bar 1%. All the data can be fitted within their experimental error bar, in the operative range $10^{-6} < W_{RJ} < 10^{-3}$.

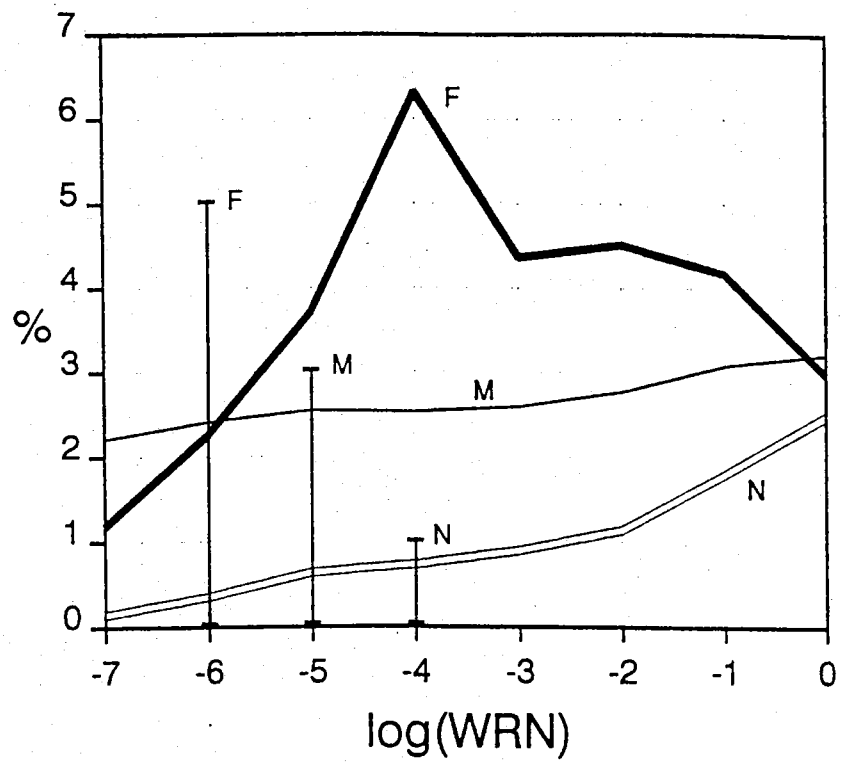

Fig. 4(b) Response of the r.m.s. fitting errors ϵ to W_{RN}, smoothness parameter of the density profile, with $W_F=10$, $W_N=10$, $W_{RJ}=10^{-5}$. The full line is for polarimetry (F), the thin line for magnetics (M) and the grey line for interferometry (N).

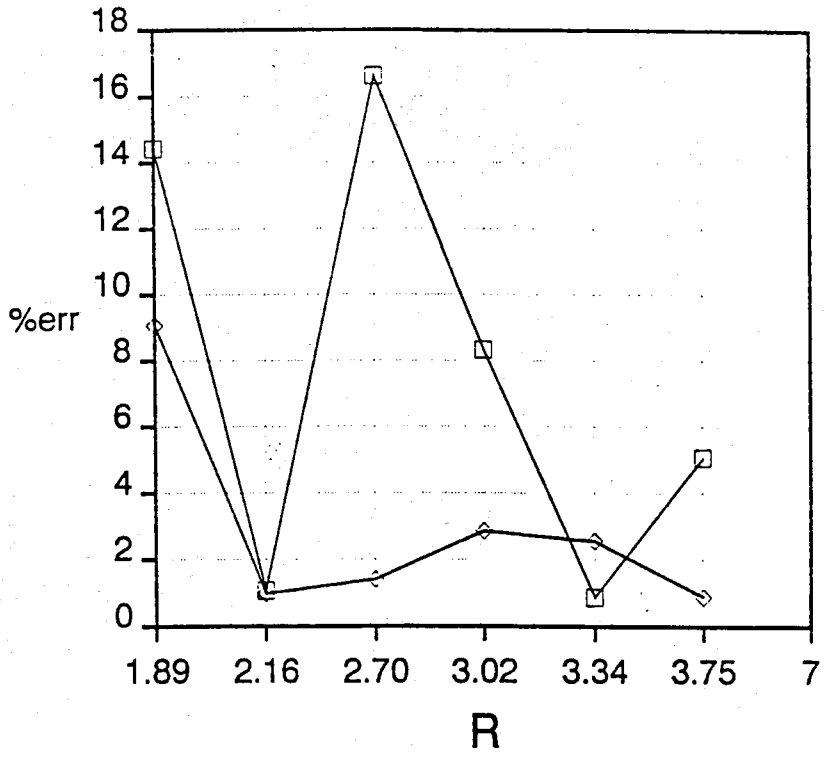

Fig. 4(c) Local fitting error (%) of Faraday data versus major radius R for [ ] magnetic data alone, < > magnetic and Faraday data.

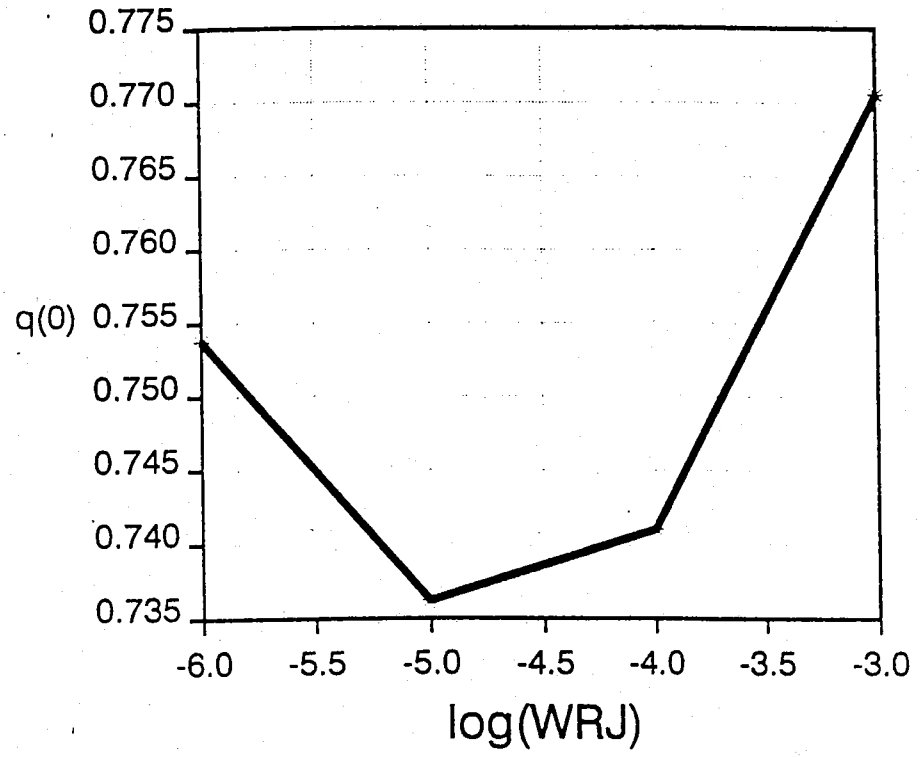

Fig. 4(d) Sensitivity of physical results to the smoothness of the current profile: q (0) versus W_{RJ}. The maximum variation of q (0) over the operative range (bias of the model) is 4.5% ($W_F=10$, $W_N=10$, corresponding to experimental standard deviations).

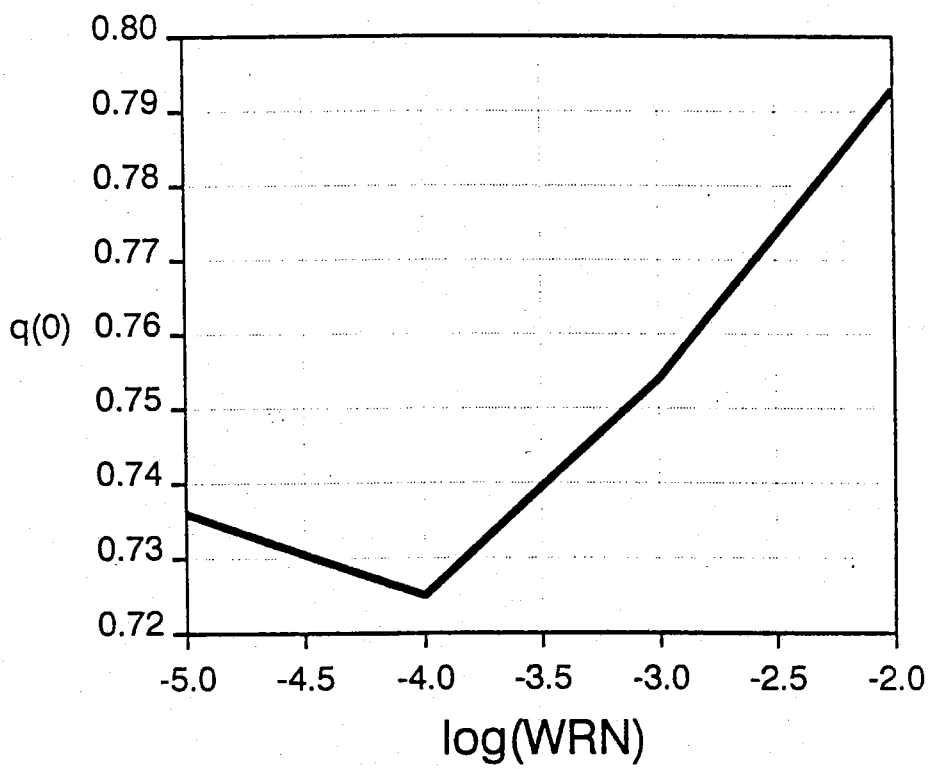

Fig. 4(e) Sensitivity of q (0) to the smoothness of the density profile. q (0) versus W_{RN}. Maximum variation of q (0) $\cong$ 8.8%.

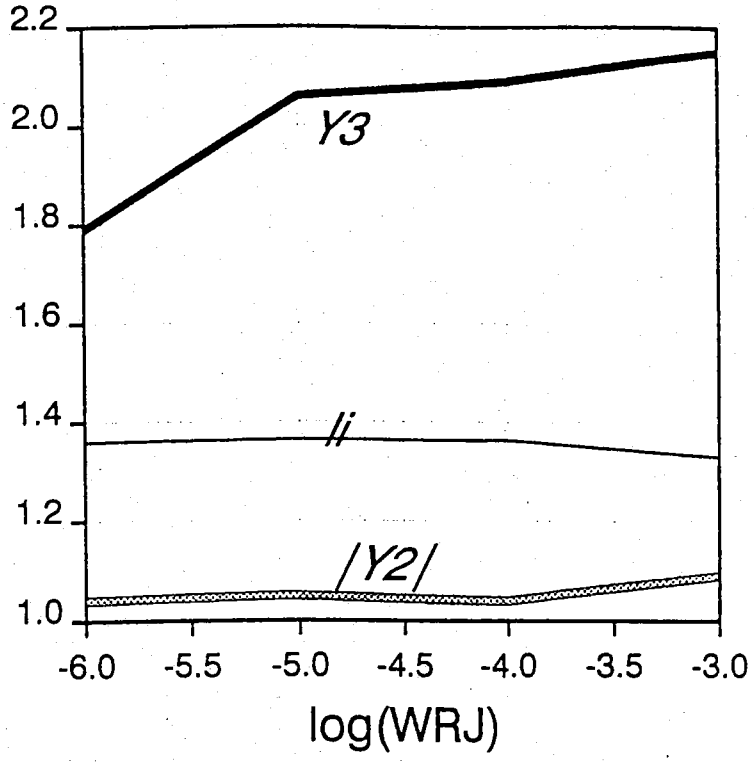

Fig. 4(f) Sensitivity to W_{RJ} of the internal inductance ℓ_i and the Shafranov current moments $10|Y_2|$, $100\ Y_3$.

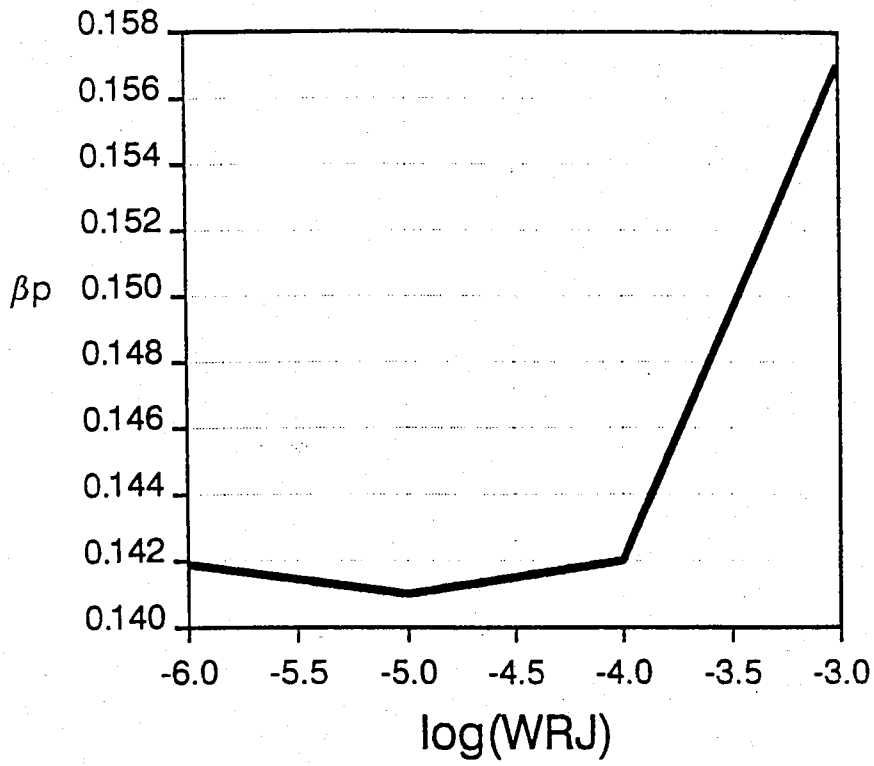

Fig. 4(g) Sensitivity of β_p, to W_{Rj}.

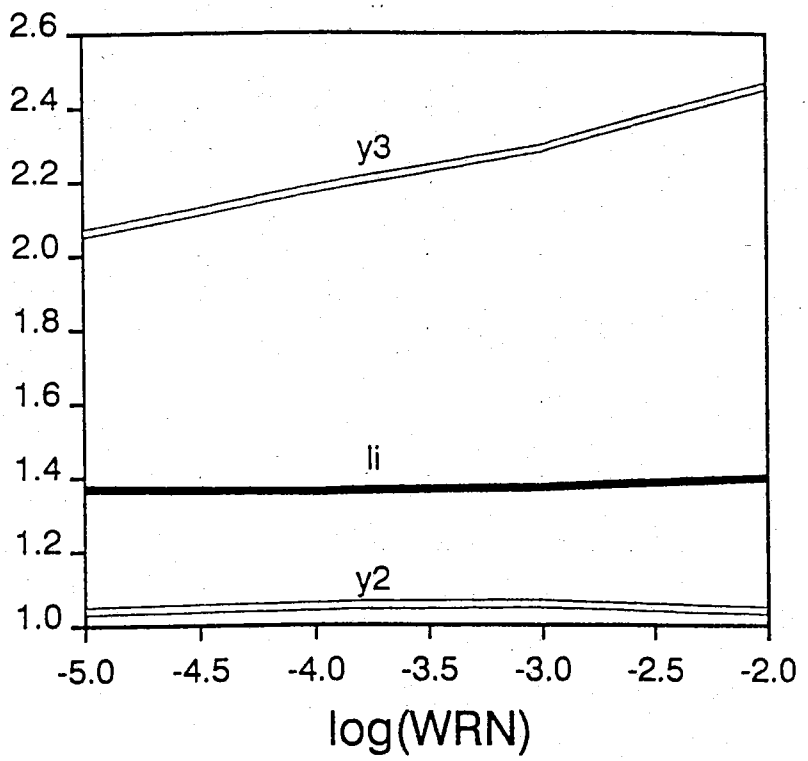

Fig. 4(h) Sensitivity to W_{RN} of ℓ_i and $10|Y_2|.100\ Y_3$.

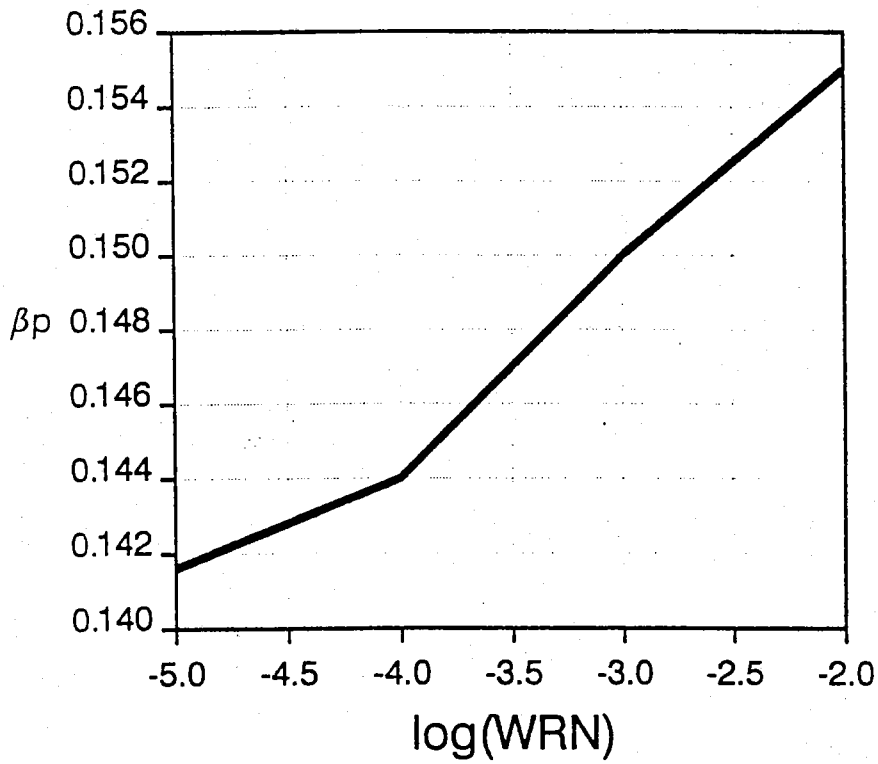

Fig. 4(i) Sensitivity of β_p to W_{RN}.

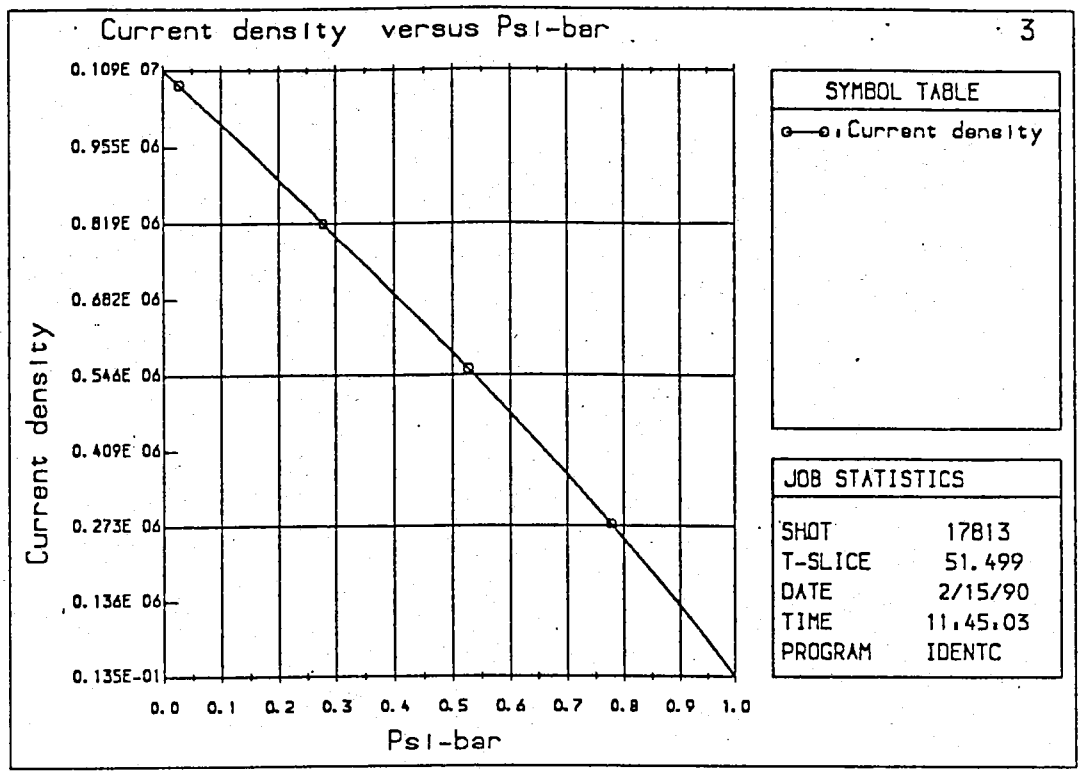

Fig. 5(a) Average current profile $<J_\phi>$ identified using $W_{RJ}=1.0$.

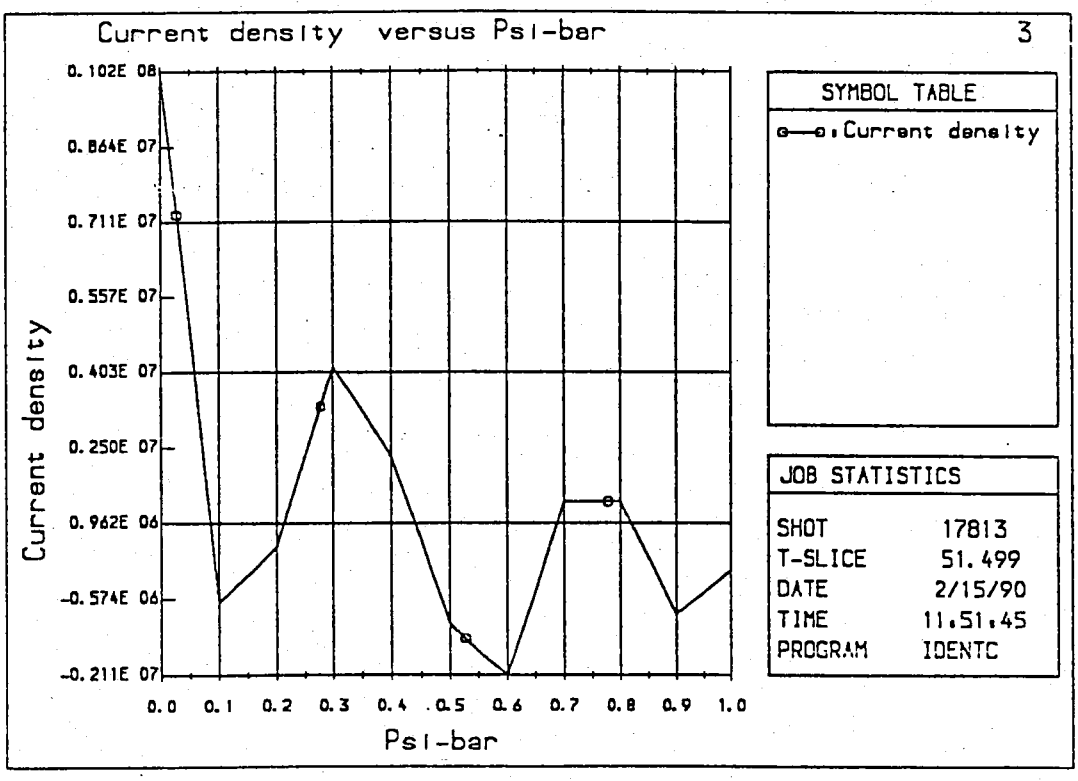

Fig. 5(b) Same as Fig. 5(a) but with $W_{Rj}=10^{-7}$.

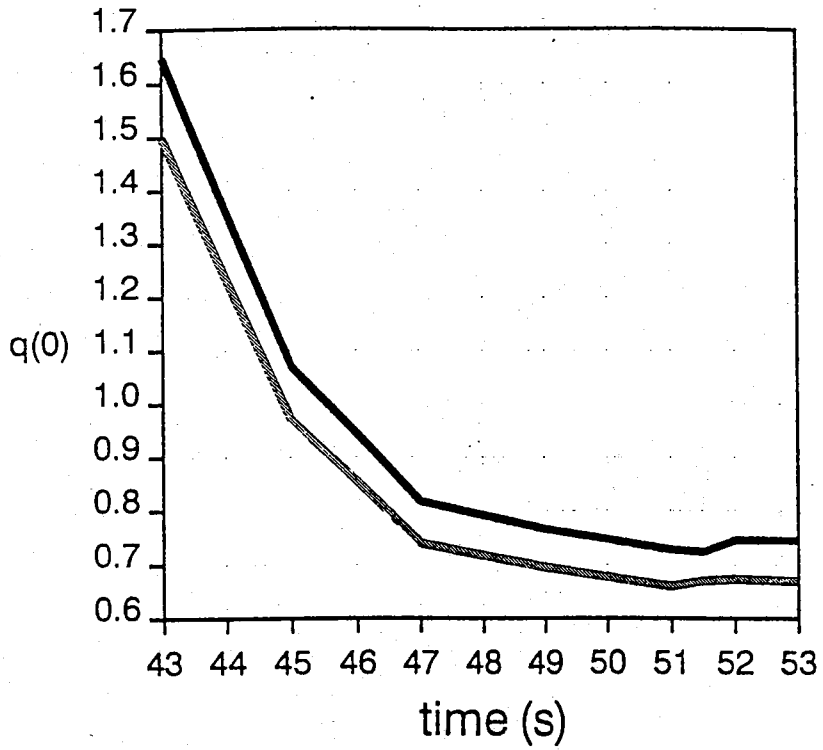

Fig. 6 Time evolution of q (0) over 10sec (shot 17813). Sawtoothing starts at t=45 when q (0) ~ 1. The full line is obtained from 'exact' data. The grey line is obtained adding a 5% systematic error to the Faraday data.

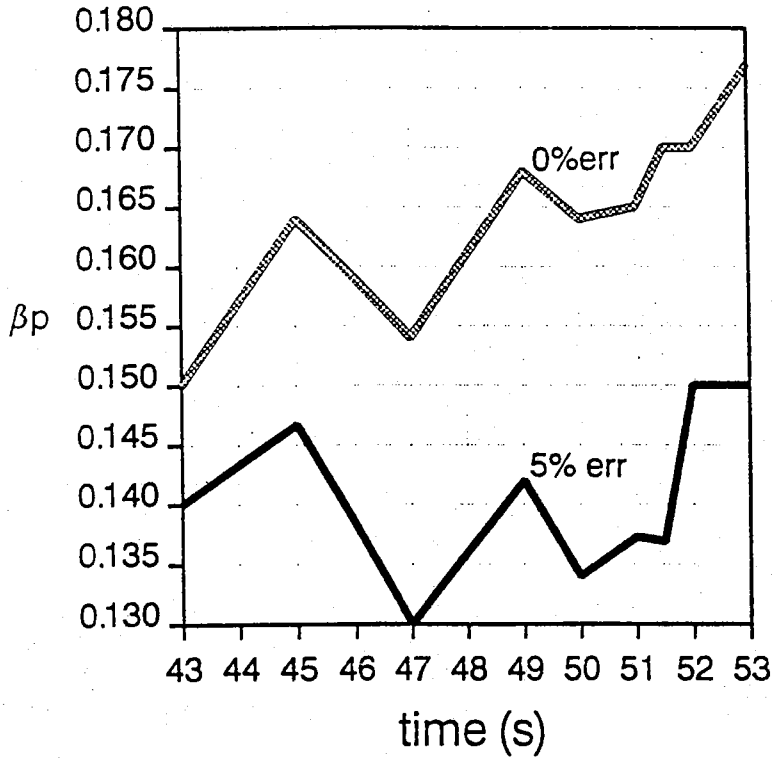

Fig. 7(a) Time evolution of β_p with exact and perturbed data as in Fig. 6.

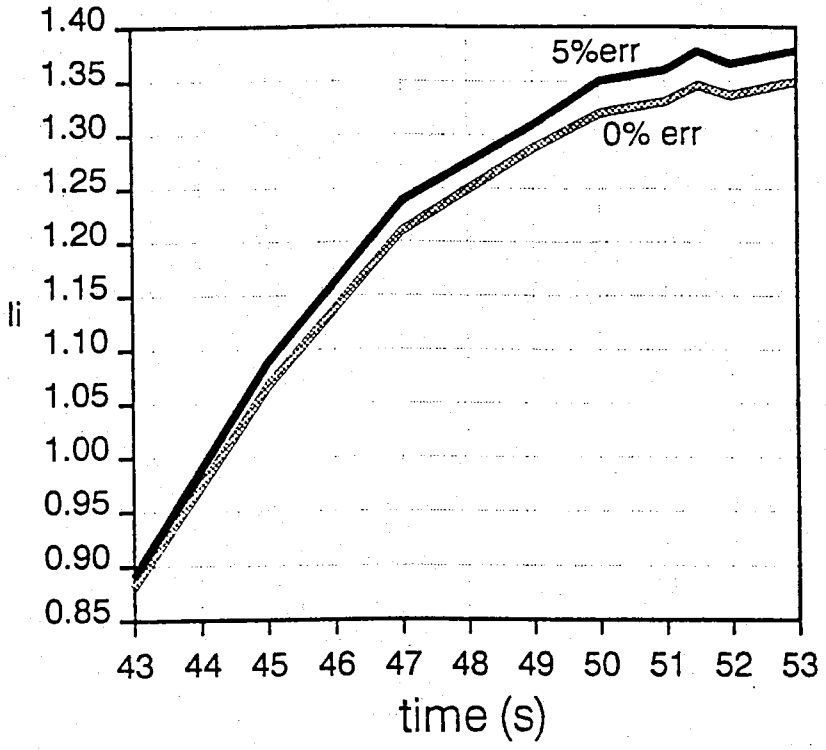

Fig. 7(b) Time evolution of ℓ_i in the same conditions as of Fig. 7(a).

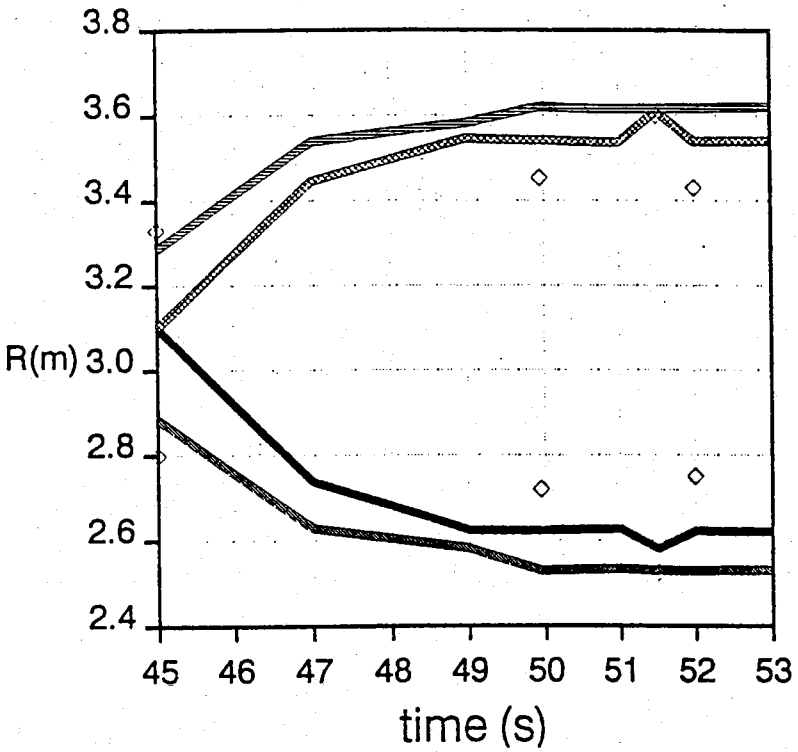

Fig. 7(c) Comparison of the position and width of $q=1$ surface with X-ray sawteeth inversion radius. The innermost and outermost major radii of the $q=1$ surface are shown for 'exact' data (full and chequered lines) and for 5% systematic perturbation (grey lines). The X-ray inversion radius position is marked by diamonds.

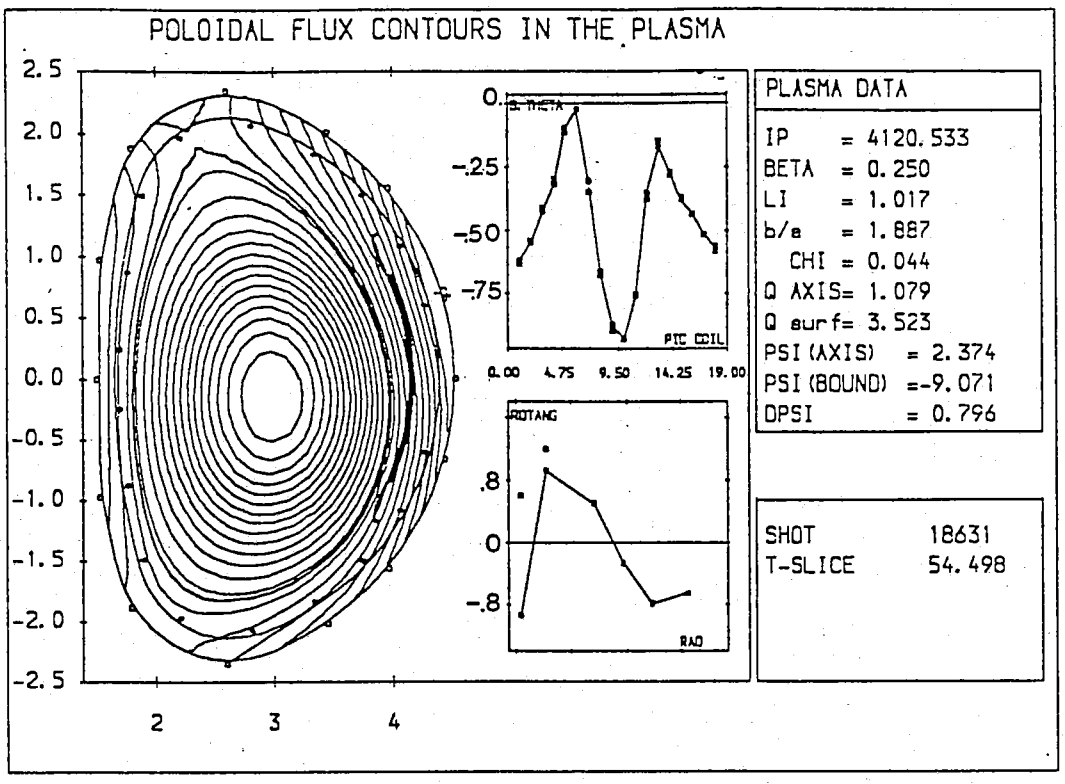

Fig. 8(a) Equilibrium reconstruction from magnetic and polarimetric data of a single X-point JET H-mode (# 18631). Two channels not operative.

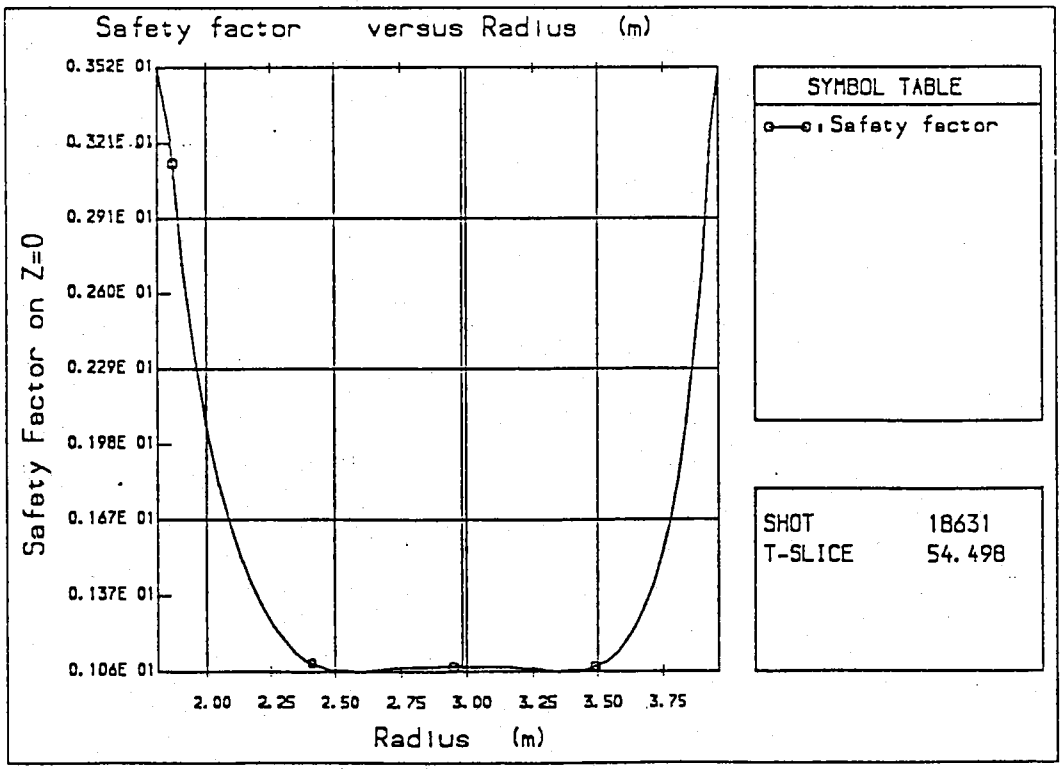

Fig. 8(b) Safety factor profile q (R) for # 18631.

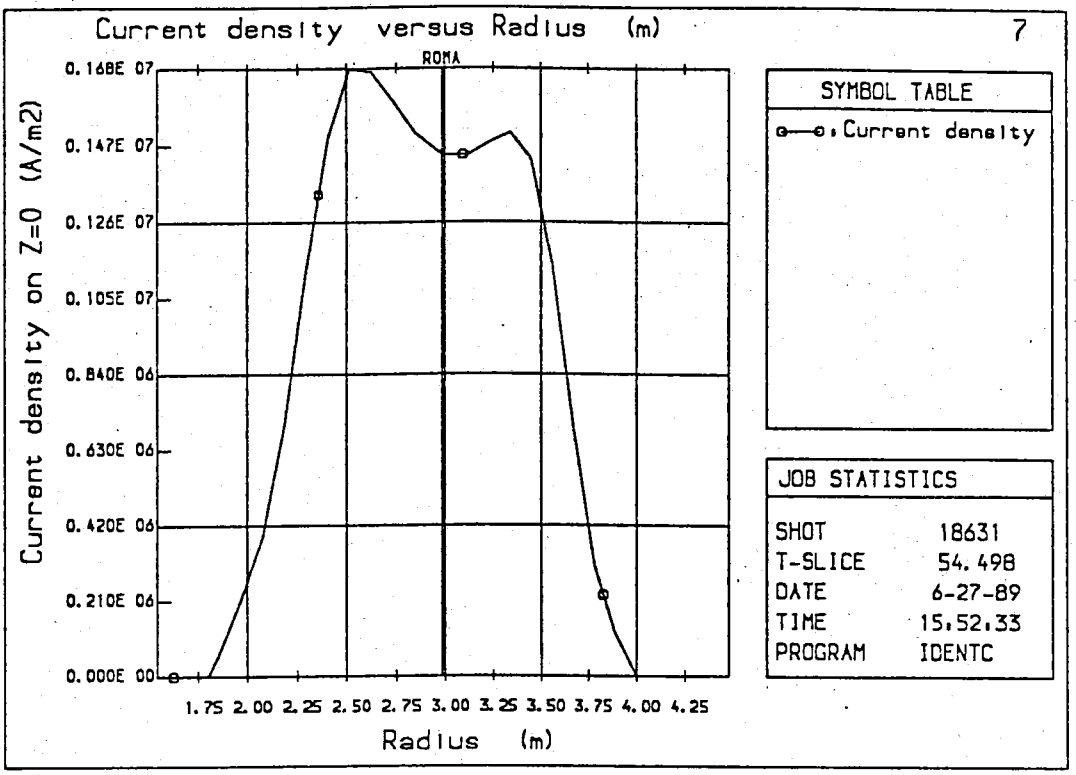

Fig. 8(c) Current density profile J_ϕ (R, $Z=0$) for # 18631.

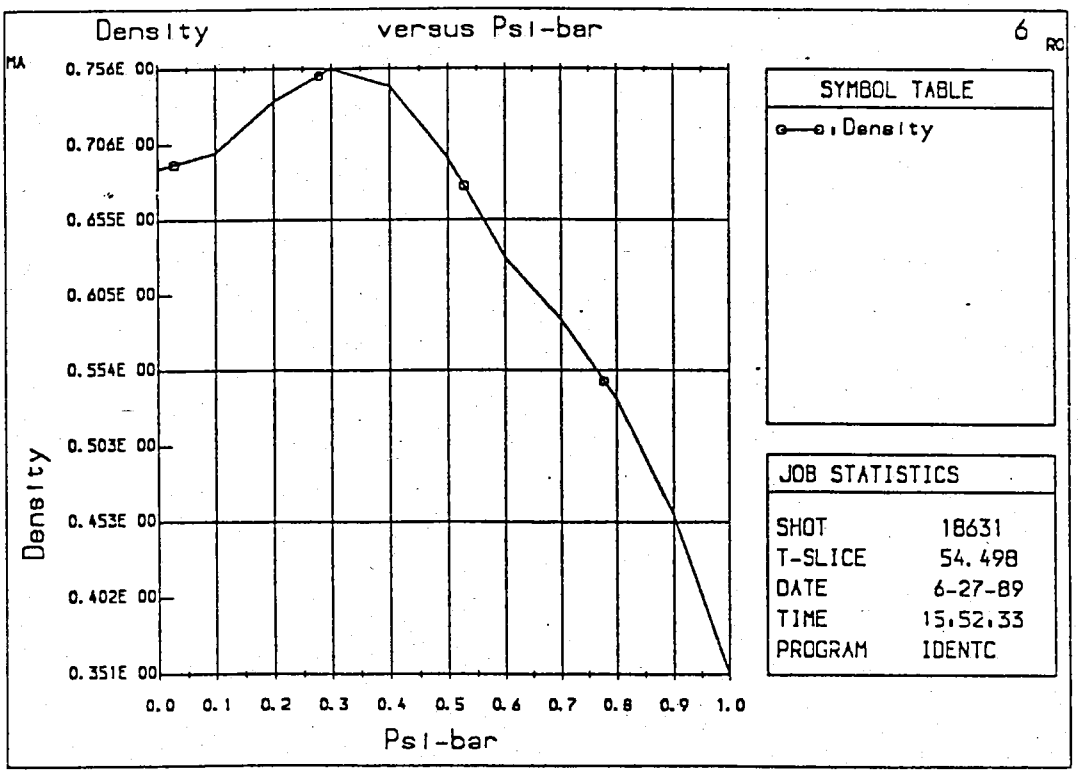

Fig. 8(d) Particle density profile n ($\bar{\Psi}$) for # 18631.

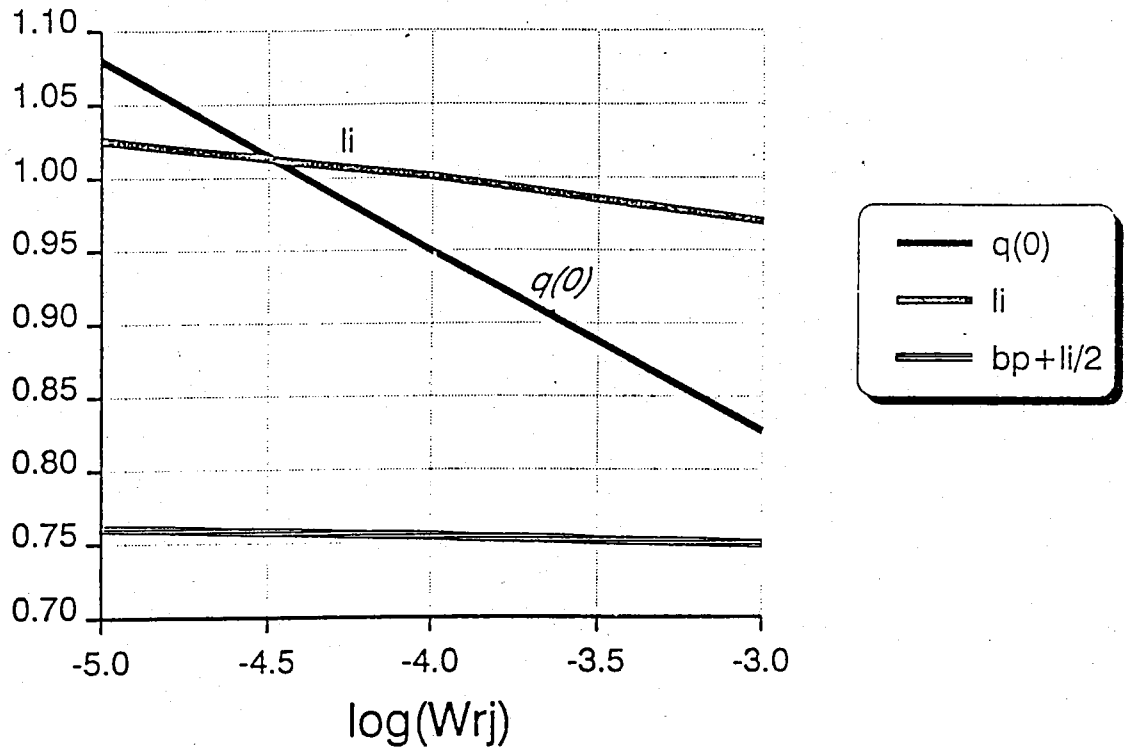

Fig. 9(a) Sensitivity of ℓ_i, q (0), $\beta_p + \ell_i/2$ to W_{RJ} (# 18631).

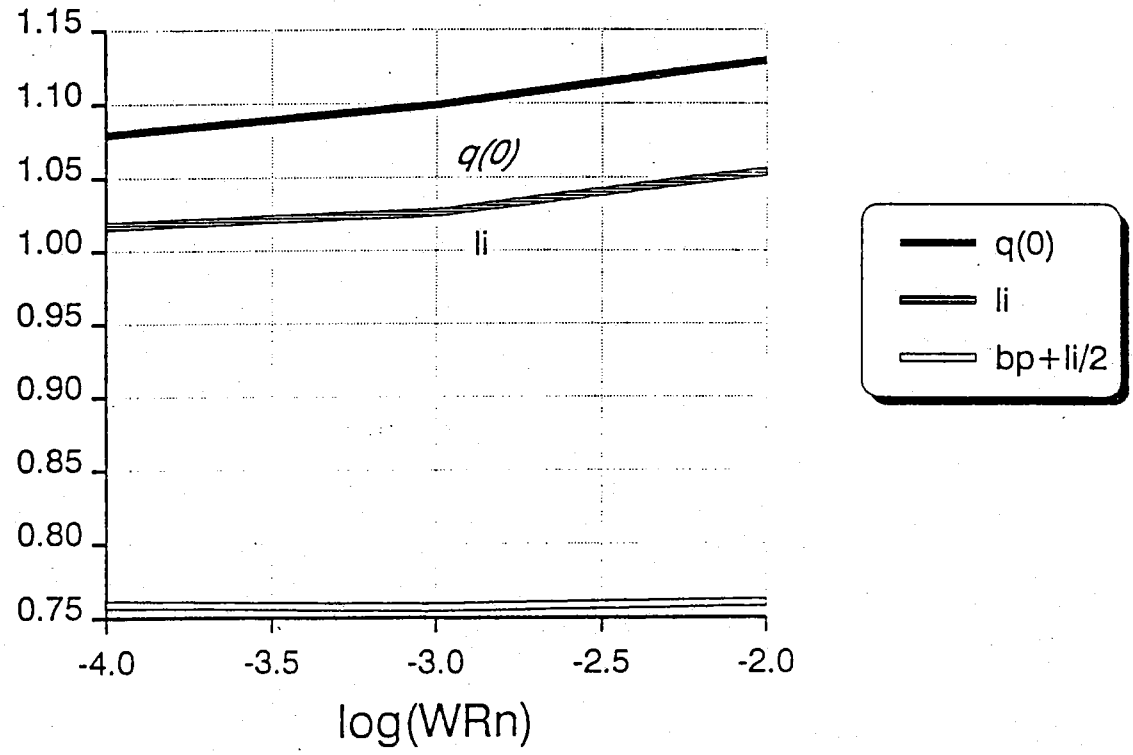

Fig. 9(b) Sensitivity of ℓ_i, to $\beta_p + \ell_i/2$ to W_{RN} (# 18631).